

A dynamic microbial sulfur cycle in a serpentinizing continental ophiolite

Mary C. Sabuda^{1†,‡}, William J. Brazelton,²
Lindsay I. Putman,^{1,3} Tom M. McCollom,⁴
Tori M. Hoehler,⁵ Michael D. Y. Kubo,^{5,6}
Dawn Cardace⁷ and Matthew O. Schrenk^{1,3*}

¹Department of Earth and Environmental Sciences,
Michigan State University, East Lansing, MI, 48824.

²Department of Biology, University of Utah, Salt Lake
City, UT, 84112.

³Department of Microbiology and Molecular Genetics,
Michigan State University, East Lansing, MI, 48824.

⁴Laboratory for Atmospheric and Space Physics, UCB
600, University of Colorado-Boulder, Boulder, CO,
80309.

⁵Exobiology Branch, NASA Ames Research Center,
Moffett Field, CA, 94035.

⁶SETI Institute, Mountain View, CA, 94043.

⁷Department of Geosciences, University of Rhode
Island, Kingston, RI, 02881.

Summary

Serpentinization is the hydration and oxidation of ultramafic rock, which occurs as oceanic lithosphere is emplaced onto continental margins (ophiolites), and along the seafloor as faulting exposes this mantle-derived material to circulating hydrothermal fluids. This process leads to distinctive fluid chemistries as molecular hydrogen (H₂) and hydroxyl ions (OH⁻) are produced and reduced carbon compounds are mobilized. Serpentinizing ophiolites also serve as a vector to transport sulfur compounds from the seafloor onto the continents. We investigated hyperalkaline, sulfur-rich, brackish groundwater in a serpentinizing continental ophiolite to elucidate the role of sulfur compounds in fuelling *in situ* microbial activities. Here we illustrate that key sulfur-cycling taxa, including *Dethiobacter*, *Desulfispora* and ‘*Desulforudis*’, persist throughout this extreme

environment. Biologically catalysed redox reactions involving sulfate, sulfide and intermediate sulfur compounds are thermodynamically favourable in the groundwater, which indicates they may be vital to sustaining life in these characteristically oxidant- and energy-limited systems. Furthermore, metagenomic and metatranscriptomic analyses reveal a complex network involving sulfate reduction, sulfide oxidation and thiosulfate reactions. Our findings highlight the importance of the complete inorganic sulfur cycle in serpentinizing fluids and suggest sulfur biogeochemistry provides a key link between terrestrial serpentinizing ecosystems and their submarine heritage.

Introduction

Serpentinization is a geochemical reaction that occurs following the exposure of ultramafic rock to hydrothermal fluid. This occurs in numerous locations around the world as oceanic lithosphere is subducted into the mantle, altered in mid-ocean ridge settings, or is emplaced onto continents in the form of ophiolites (Dilek and Furnes, 2011; Morrill *et al.*, 2013). Detachment faulting on the ocean floor can also uplift ultramafic rock and facilitate the interaction of water and rock at elevated temperatures (Schwarzenbach *et al.*, 2016). At temperatures below ~300°C, the pH of these systems ranges from 7.5 to greater than 12.5. Subsurface serpentinizing fluids, such as those at the Coast Range ophiolite in California and the Semail ophiolite in Oman, are often dysoxic to suboxic [2.36–0.09 mg L⁻¹ dissolved oxygen (DO) at Coast Range Ophiolite Microbial Observatory (CROMO)] due to their increased isolation from atmospheric and surface processes with depth (Morrill *et al.*, 2013; Schrenk *et al.*, 2013; Rempfert *et al.*, 2017; Twing *et al.*, 2017; Fones *et al.*, 2019). Serpentinizing springs exposed to the atmosphere can host gradients of oxygen from anoxic at the source to fully oxygenated and therefore more energy-rich as water moves downstream (Woycheese *et al.*, 2015). Serpentinization-influenced microbial ecosystems have stimulated a great deal of interest in recent years following the discovery of the Lost City Hydrothermal Field (LCHF) near the Mid-Atlantic Ridge and the

Received 8 June, 2019; revised 19 March, 2020; accepted 30 March, 2020. *For correspondence. E-mail schrenkm@msu.edu; Tel. (517) 884 7966 Present addresses: [†]Department of Earth and Environmental Sciences, University of Minnesota - Twin Cities, Minneapolis, MN 55455, USA; [‡]BioTechnology Institute, University of Minnesota – Twin Cities, St. Paul, MN 55108, USA.

exploration of numerous serpentinizing ophiolite complexes (Brazelton *et al.*, 2012; Schrenk *et al.*, 2013; Tiago and Veríssimo, 2013; Suzuki *et al.*, 2014). Microorganisms within these habitats are able to metabolize products of serpentinization (Lang *et al.*, 2012; Quéméneur *et al.*, 2014) and facilitate biogeochemical cycling of the limited substrates (i.e., hydrogen, methane, acetate and formate) and electron acceptors (nitrate, sulfate, iron, etc.) that are present therein. Owing to their marine origins, some ophiolite-hosted aquifers retain ancient seawater, which contributes salinity and dissolved sulfate to the chemical inventory (Fig. 1; Supporting Information Tables S1 and S2) and may influence microbial community structure (Schwarzenbach *et al.*, 2012).

Previous studies have identified some evidence of organisms capable of metabolizing sulfur compounds within serpentinizing ecosystems through pathways that include dissimilatory sulfate reduction, polysulfide reduction and sulfide oxidation (Brazelton *et al.*, 2006; Crespo-Medina *et al.*, 2014; Lang *et al.*, 2018). Organisms similar to *Dethiobacter* were enriched when anoxic serpentinizing groundwater was amended with thiosulfate and sulfide (Crespo-Medina *et al.*, 2014). At Cabeço de Vide in Portugal, a high pH aquifer influenced by serpentinization, microbial communities and functional

gene markers suggest that inorganic sulfur metabolisms (e.g., *aprA*) play a key role in the subterranean ecosystem (Tiago and Veríssimo, 2013). However, the contributions of these individual metabolic processes to bulk ecosystem function have not been well defined. Here, we use a combination of thermodynamic and metagenomic approaches to address the roles of inorganic sulfur in oxidized (sulfate), reduced (sulfide) and intermediate (thiosulfate, sulfite, polysulfides, elemental sulfur) oxidation states in stimulating microbial metabolic activity within a serpentinite-hosted aquifer at CROMO in California, USA. Gibbs energy yields for catabolic reactions involving dissolved sulfur compounds were calculated using the measured geochemistry of CROMO groundwater (Amend and Shock, 2001; Cardace and Hoehler, 2009). We then quantified the abundance and expression of key sulfur cycling genes in metagenomes and metatranscriptomes from resident microbial communities. These genes and their phylogenetic affiliation were used to construct a model of sulfur cycling in the deepest, most saline groundwater well at the site, CSWold. Finally, the genetic potential for sulfur cycling at CROMO is compared to metagenomes from other serpentinization-influenced sites including the Voltri Massif in Italy and the LCHF to investigate the distribution of commonly

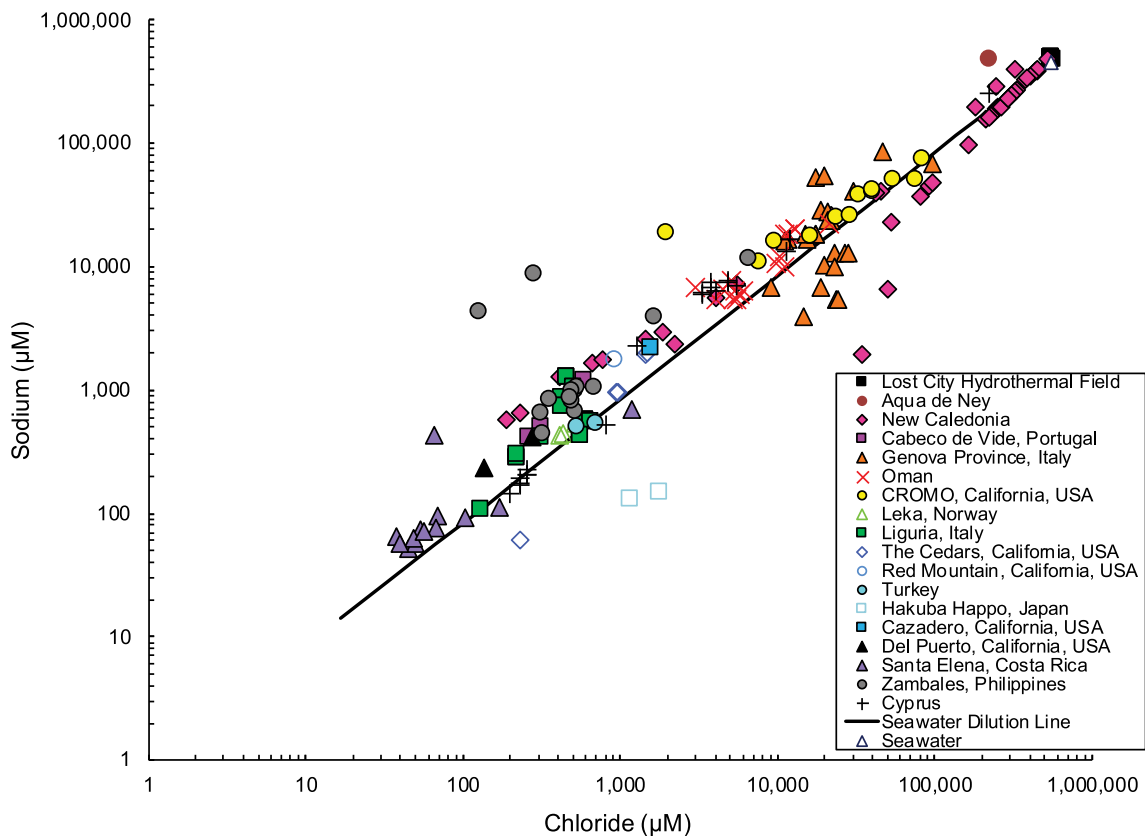


Fig. 1. Sodium and chloride values (μM) are plotted for published subaerial serpentinizing systems worldwide (see Supporting Information Table S2), with a seawater dilution line (black) plotted for reference. CROMO wells plot as yellow circles.

occurring processes. These data were used to explore the idea that microbial sulfur cycling at CROMO represents part of a continuum of processes that occur as serpentinites transition between marine and terrestrial environments.

Results and discussion

Aqueous geochemistry and microbial community patterns at CROMO

CROMO consists of eight monitoring wells drilled into the northern Coast Range ophiolite in 2011 along with four pre-existing wells. The wells access a dysoxic ($0.66\text{--}2.96\text{ mg O}_2\text{ L}^{-1}$) to suboxic ($0.03\text{--}0.66\text{ mg O}_2\text{ L}^{-1}$) aquifer containing some of the most saline serpentinite-hosted groundwater characterized to date (Fig. 1, Supporting Information Tables S1 and S2). Earlier

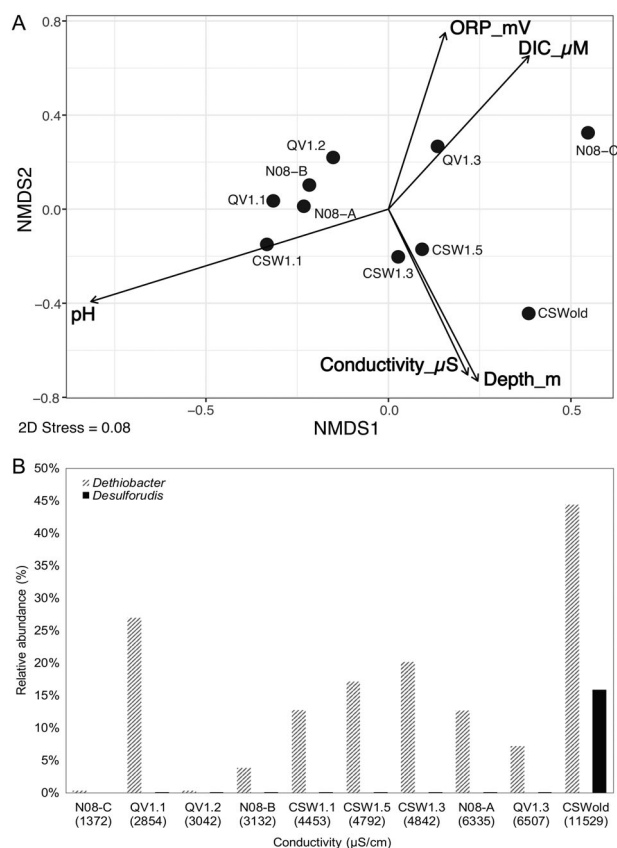


Fig. 2. A. Non-metric multidimensional scaling (NMDS) plot of CROMO well 16S rRNA gene amplicon relative abundances using the Morisita Horn distance metric, with correlations to select geochemical data plotted as overlying vectors (p values ≤ 0.05). Wells clustered closely are more similar in microbial community structure than those further away.

B. Bar chart showing 16S rRNA relative gene abundance (%) of two genera, *Dethiobacter* and *Desulfuridis*, versus conductivity ($\mu\text{S cm}^{-1}$) in CROMO wells. Wells are ordered from lowest to highest conductivity.

hydrologic studies have suggested the presence of perched aquifers at CROMO, which isolate fluid volumes at specific depths from one another (Ortiz *et al.*, 2018). The wells are geographically split into two clusters, Core Shed Wells (CSW) and Quarry Valley wells (QV, N08) located 1.2 km apart (Cardace *et al.*, 2013). The deepest wells ($> 27\text{ m}$) access microbial communities minimally influenced by surficial processes (i.e., meteoric water, soil organics, etc.). Work by Peters (1993) revealed that Coast Range ophiolite groundwater is partially derived from Cretaceous seawater that experienced varying extents of water–rock interaction. The deepest wells host fluid salinities an order of magnitude higher than the shallowest wells and are elevated (e.g., 81.9 mM Cl^- and 73.9 mM Na^+ in CSWold) compared to most measured continental serpentinitizing sites such as the Cedars (1.49 mM Cl^- and 1.98 mM Na^+ at site BS5; Morrill *et al.*, 2013) and the Semail ophiolite (21.1 mM Cl^- and 22.1 mM Na^+ at site Yellowstone du pauvre; Chavagnac *et al.*, 2013; Supporting Information Fig. S1, Table S2). Deeper wells plot along the $\text{Na}^+\text{-Cl}^-$ seawater dilution line rather than the 1:1 halite dissolution line (Supporting Information Fig. S1), which suggests the deepest wells sample groundwater with a dilute seawater signature (Hem, 1985; Alcalá and Custodio, 2008; Katz *et al.*, 2011). In the deepest well, CSWold (depth = 76.2 m), some of the most abundant organisms as identified by 16S rRNA gene sequencing are closely related to halotolerant and halophilic taxa, including members of the genera *Salinarimonas*, *Desulfitispora* and *Nitriliruptor*. $\text{Br}^-:\text{Cl}^-$ ratios also parallel the seawater dilution trend but offset to slightly higher values (Supporting Information Fig. S2), consistent with the results of Peters (1993). The offset suggests that some Cl^- was removed from the fluid at depth, possibly through substitution of Cl^- for hydroxyl groups in serpentine or precipitated in Cl-bearing minerals such as iowaite (Helwig and Schwarz, 2007).

The seawater-influenced groundwater chemistry is coincident with several other physical–chemical parameters that co-vary with microbial community composition including oxidation–reduction potential, conductivity, depth, dissolved inorganic carbon (DIC) and pH (Fig. 2; Supporting Information Table S3). Pairwise Pearson correlation analyses between geochemical and microbiological (16S rRNA gene amplicon) data from the CROMO wells demonstrated that members of Betaproteobacteriales and Erysipelotrichales (Firmicutes) are positively correlated with the concentration of hydrogen sulfide (HS^- ranges $1.00\text{--}23.75\text{ }\mu\text{M}$; p values < 0.05 ; Supporting Information Tables S1 and S3–S5). The sulfur-reducing taxa *Dethiobacter*, *Desulfitispora*, Clostridiales Family XIV and ‘*Desulfuridis*’ also correlate with depth and conductivity (Fig. 2; Supporting Information Table S5; p values < 0.05), and well depth correlates with sodium and conductivity (Supporting Information Table S6;

p values < 0.05). While microbial populations in highly reducing, hyperalkaline groundwater are generally limited by the lack of more energy-rich electron acceptors (oxidants such as O_2 , NO_3^- and Mn; McCollom and Seewald, 2013; Twing *et al.*, 2017), the presence of dissolved sulfate here provides a resource that could be exploited by microbial communities and stimulate a range of secondary metabolisms. Overall, the cycling of sulfur in this system and in similar serpentinizing systems allows for the recycling and regeneration of limited oxidants.

Biological sulfate reduction 'kick-starts' the sulfur cycle in serpentinizing ophiolites

Sulfate sourced from ancient seawater constitutes the most abundant dissolved sulfur compound at CROMO as demonstrated both here and through earlier investigations (Peters, 1993). Sulfate in seawater is 28 mM, and sulfate ranges between 28 and 392 μ M at CROMO (Supporting Information Tables S1 and S3) and is elevated in other relatively saline ophiolites around the world (Neal and Shand, 2002; Cipolli *et al.*, 2004; Chavagnac *et al.*, 2013). Thermodynamic calculations for a range of biologically catalysed sulfate reduction reactions in CROMO's highly reducing, alkaline groundwater demonstrate favourable conditions for microbial sulfate reduction coupled to a range of potential fuels including hydrogen, methane and acetate (Schrenk *et al.*, 2013; Supporting Information Tables S7 and S8). For example, sulfate reduction coupled to acetate and formate in all wells, and to hydrogen in most wells, yields sufficient Gibbs energy (> 70 kJ mol⁻¹) to generate ATP (adenosine 5'-triphosphate; Schink, 1997). Sulfate reduction coupled to methane oxidation (anaerobic oxidation of methane (AOM)) is a highly favourable process in terms of bulk energetic yields per litre of groundwater, especially at depth (Fig. 3; Supporting Information Tables S7 and S8). In the four deepest wells, this reaction yields (per litre of groundwater) values of 6500 mJ L⁻¹ in CSWold, 13,000 mJ L⁻¹ in CSW1.5, 2100 mJ L⁻¹ in N08-A and 2100 mJ L⁻¹ in QV1.3. The shallowest wells CSW1.4 and N08-C, by comparison, have values of 100 mJ L⁻¹ and 32 mJ L⁻¹ respectively (Fig. 3, Supporting Information Tables S7 and S8). Additionally, the deepest wells at CROMO (e.g., CSWold; Supporting Information Table S9) are dominated by taxa associated with sulfate reduction, such as relatives of '*Desulfurudis audaxviator*' (11.9% relative abundance; Jungbluth *et al.*, 2017). The potential for AOM coupled to sulfate reduction has also been shown in other terrestrial serpentinites. In Oman, it is suggested that sulfate reduction coupled to methane oxidation is an energetically feasible metabolism for microbes (Miller *et al.*, 2016), and in the

Philippines, this sulfate reduction reaction yields an estimated -25 kJ mol⁻¹ on average between all wells (Cardace *et al.*, 2015) which are less than the values calculated for CROMO (Supporting Information Table S7).

Genes coding for the complete dissimilatory sulfate reduction pathway to sulfide, sulfate adenylyltransferase (*sat*), adenosine-5'-phosphosulfate reductase (*aprAB*) and dissimilatory sulfite reductase (*dsrAB*) are expressed in four wells (Fig. 4; Supporting Information Tables S10 and S11). The data demonstrate particularly elevated expression of *aprAB* genes in the deepest, most saline well, CSWold, with a Log₂ fold change of 7.38 and 6.79 for *apr A* and *B*, respectively, relative to neutral pH wells (Supporting Information Table S12). Upon examination of the contigs, metagenomic data indicate that *sat*, *aprAB* or *dsrAB* genes are not harboured on the same contig (Supporting Information Table S13). A phylogenetic analysis of a key gene in this sulfate reduction pathway, *dsrB*, illustrates the diversity of organisms capable of sulfate reduction within serpentinizing systems (Fig. 5; Supporting Information Table S14). Through comparison by NCBI BLASTP, CROMO *dsrB* genes closely match those from known sulfate-reducing bacteria such as *Desulfitibacter alkalitolerans* (98.04%) and *Thermodesulfovibrio thiophilus* (77.84%). The oxidative function of *dsrB* is also represented in the distribution of genes in continental ophiolites, including some wells of the CROMO site, and is primarily affiliated with Betaproteobacteria (Fig. 5). *PhyloPythiaS+* results confirm that CROMO contigs containing *dsr* closely match sulfate-reducing members of the Firmicutes, Betaproteobacteria and Deltaproteobacteria (Supporting Information Table S13; Fig. 5; Müller *et al.*, 2015; Gregor *et al.*, 2016), and metatranscriptome data indicate that *dsr* is actively transcribed to various extents in all wells analysed (Fig. 4).

Metagenome-assembled genomes (MAGs) created from these data (described and reported extensively in Seyler *et al.*, 2020) show that the capability to mediate different sulfur metabolisms was segregated into different taxonomic groups. Of the most abundant organisms in CSWold (Supporting Information Table S9), three MAGs within the Clostridiales, related to the Candidate genus *Desulfurudis*, contained genes associated with the key components of the dissimilatory sulfate reduction pathways, *dsrAB* and *aprAB*. Two MAGs related to the Peptococcaceae (related to *Desulfitispora*) and five MAGs related to *Dethiobacter alkaliphilus* contained genes involved in thiosulfate disproportionation and sulfur reduction (e.g., sulfur transferases) but lacked components involved in sulfate reduction, as has been observed in previous studies (Melton *et al.*, 2017). This may be a consequence of a low degree of completeness in these bins or due to the presence of novel genetic variants. Finally, three MAGs related to the genus *Hydrogenophaga* (i.e., *Serpentinomonas*) and two MAGs

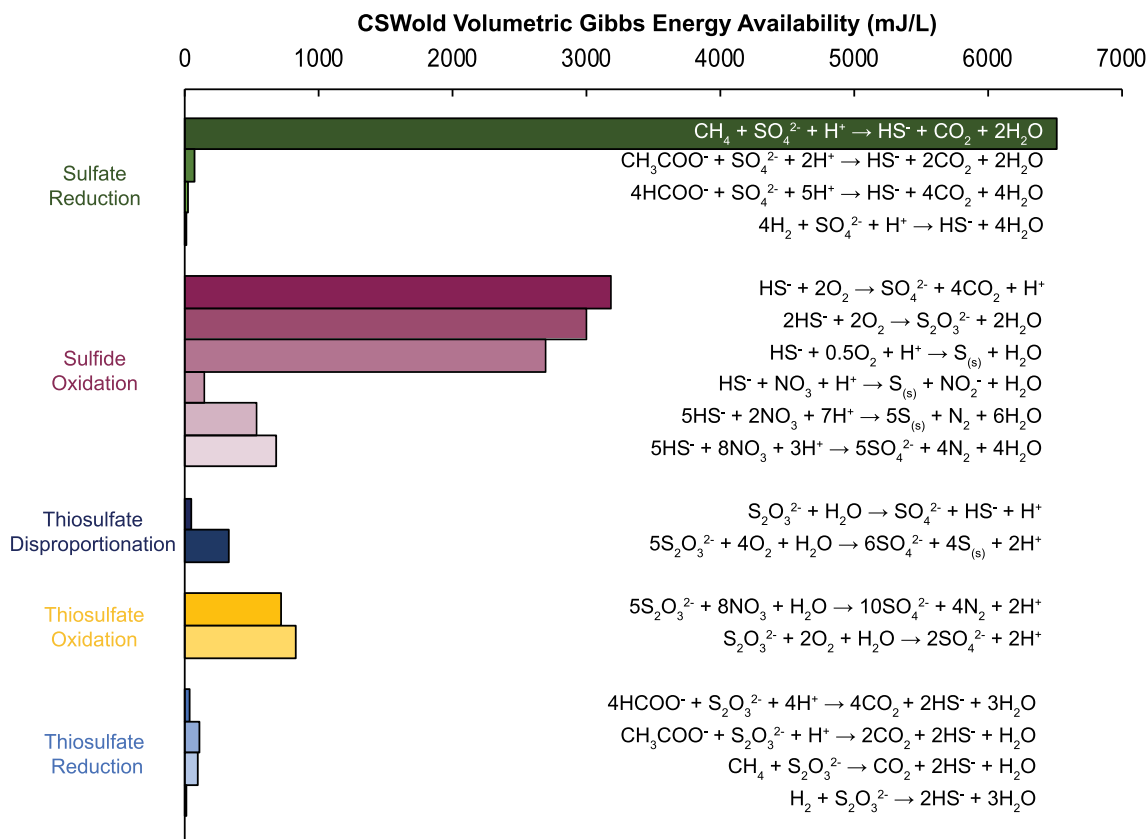


Fig. 3. Millijoules of energy available per litre of fluid for a suite of sulfur reactions. Calculations were made using measured aqueous geochemistry data in Supporting Information Table S1 for specific sulfur reactions listed in Supporting Information Table S7 within the deepest, most saline well CSWold. [Color figure can be viewed at wileyonlinelibrary.com]

within the Rhodobacteraceae had several of the key genes involved in thiosulfate oxidation via the SOX pathway. These organisms are presumed to mediate oxidative portions of the sulfur cycle at CROMO.

Taken together, these data indicate that microbial communities inhabiting brackish, hyperalkaline groundwater at CROMO have both the genetic and bioenergetic potential to carry out dissimilatory sulfate reduction. Members of Deltaproteobacteria and Clostridia, among others, have genes for sulfate reduction (Fig. 6; Supporting Information Table S13) and may be the primary drivers of this process in deeper wells, which parallels the predicted role of sulfur compounds in other deep biosphere ecosystems (Chivian *et al.*, 2008; Osburn *et al.*, 2014; Lau *et al.*, 2016).

Sulfide oxidation and production of intermediate sulfur compounds

Hydrogen sulfide (HS^-) comprises a second major sulfur pool at CROMO, and ranges from 1 μM in shallower wells up to 24 μM in deeper wells (Supporting Information Table S1). Sulfide is generally more reactive than sulfate, and the abiotic oxidation of sulfide to sulfate or

thiosulfate occurs readily at 25°C under oxic conditions (Van Den Bosch *et al.*, 2008; Luther *et al.*, 2011). Thus, sulfide is unlikely to be retained during ophiolite emplacement, and microbial activities in the host materials are only expected to accelerate this process. Between the lability of dissolved sulfide compounds and evidence for active sulfate reduction indicated through metagenomic and metatranscriptomic data (Fig. 4), it is expected that the hydrogen sulfide measured in CROMO groundwater is mainly the result of sustained active biological sulfate reduction.

Thermodynamic calculations show that sulfide oxidation to sulfate coupled to nitrate or oxygen reduction is generally favourable throughout the system but increases in volumetric energy availability (mJ L^{-1}) towards deeper areas (Supporting Information Table S7). The HS^- produced by sulfate reduction can also be partially oxidized to intermediate species such as thiosulfate ($\text{S}_2\text{O}_3^{2-}$) and elemental sulfur (S^0) via abiotic and biotic pathways. Metagenomic data indicate that the metabolic potential exists in these deeply seated fluids to oxidize sulfide to produce sulfate and sulfur intermediates (Fig. 4; Supporting Information Tables S10 and S11). At

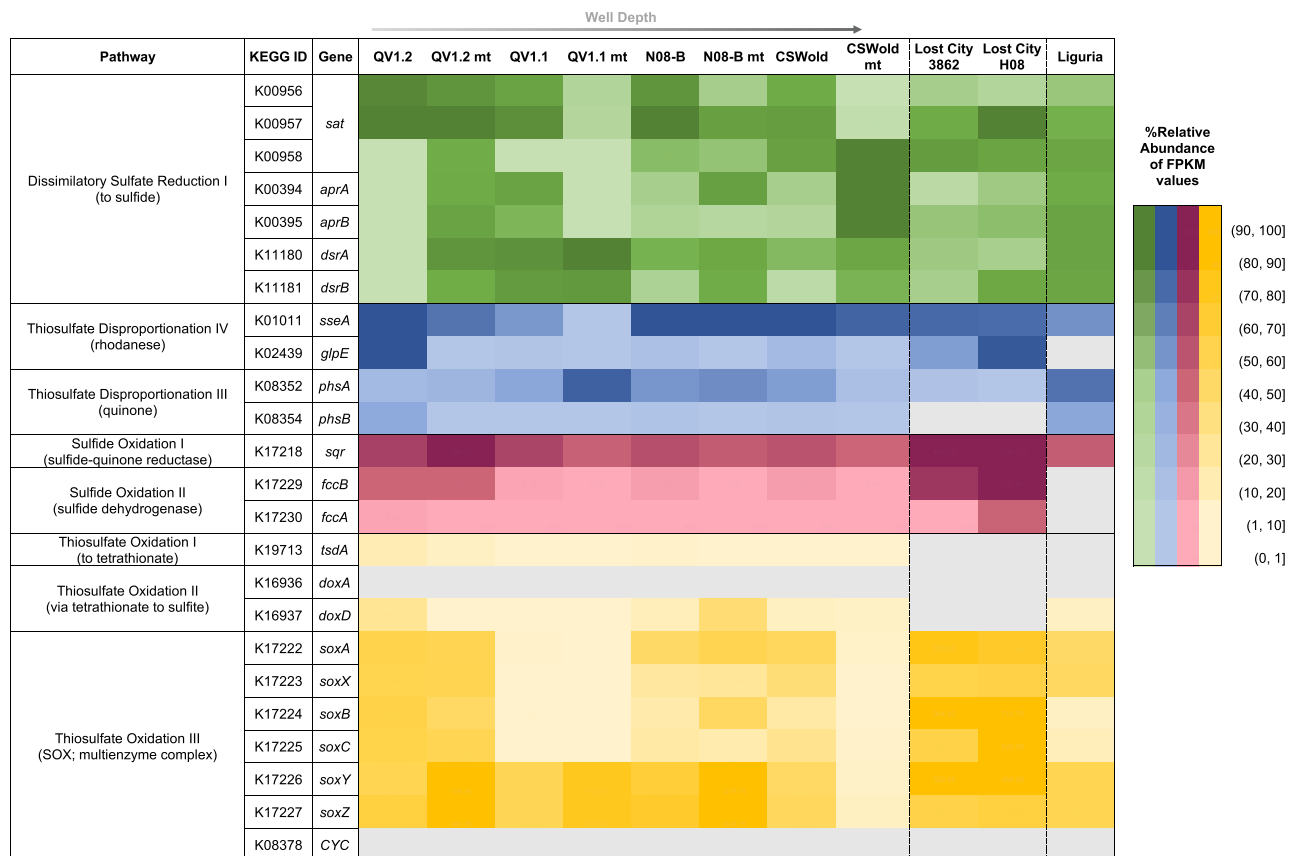


Fig. 4. The eight sulfur catabolic pathways are listed on the y-axis with their respective KEGG accessions and gene names for CROMO, Lost City and Liguria. Metagenomic and metatranscriptomic data are plotted on the heatmap as metagenome fragments per kilobase of predicted protein sequence per million mapped reads (FPKM). Metatranscriptomes are listed next to the metagenome abundance for each site using the abbreviation, mt. Each box contains a discrete FPKM value (listed in Supporting Information Tables S10 and S11), which is conditionally formatted to be colour coded by value. Intensity of a certain colour relates to the FPKM of each gene detected in a well relative to the highest FPKM value measured within the given set of metabolic pathways. Grey fill indicates no sequences met the given criteria.

CROMO, metagenomic data suggest that the sulfide oxidation I pathway (featuring the sulfide-quinone reductase enzyme, *Sqr*) is the dominant way by which organisms metabolize sulfide (Fig. 4), which results in the formation of elemental sulfur (Thorup and Schramm, 2017) and polysulfides (Wasmund *et al.*, 2017). Metatranscriptomic values (reported as FPKM) for *sqr* in the sulfide oxidation I pathway are 395.21, 31.97, 61.92 and 10.61 for QV1.2, QV1.1, N08-B and CSWold respectively (Supporting Information Table S10). At high pH, sulfide can attack elemental sulfur to form polysulfides, which are then chemically stable (Van Den Bosch *et al.*, 2008; Sousa *et al.*, 2018). Elemental sulfur can be biologically disproportionated into $S_2O_3^{2-}$ and HS^- to regenerate these reactive components (Fig. 6). A precise description of biogeochemical processes related to sulfur cycling in serpentinites is clouded by the recycling and production of intermediate sulfur compounds (e.g., thiosulfate, sulfite, elemental sulfur, polysulfides). However, once sulfur

intermediates are produced, a range of both chemical and biological transformations becomes possible.

Microbial cycling of intermediate sulfur compounds

Thiosulfate ($S_2O_3^{2-}$) is an intermediate sulfur compound that provides an important link connecting many sulfur metabolic pathways. Previous work in sulfur-rich anoxic marine and freshwater sediments has shown that thiosulfate is key to coupling oxidative and reductive pathways of the sulfur cycle (e.g., Jorgensen, 1990). Here, metagenomic data suggest a similar role in hyperalkaline groundwater (Fig. 4). Within serpentinizing systems, thiosulfate is rarely discussed in studies of sulfur cycling (Leavitt *et al.*, 2014; Suzuki *et al.*, 2014). Explicit measurements of thiosulfate for serpentinizing systems have yet to be performed, including in the present study. Given the important role of thiosulfate suggested by CROMO metagenomic data, thermodynamic calculations performed across a six-order of magnitude range of

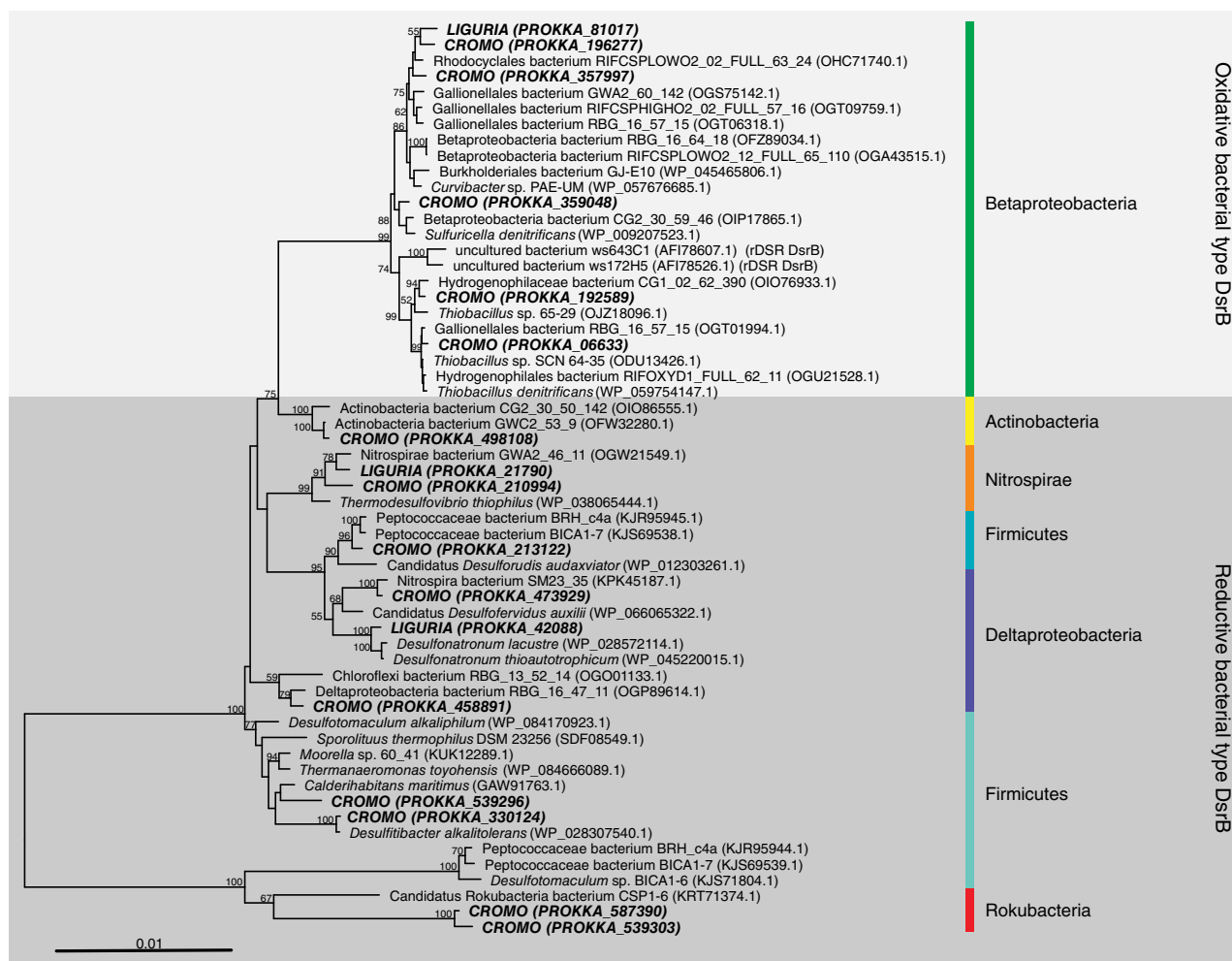


Fig. 5. A 1000-bootstrap maximum likelihood phylogenetic tree of CROMO and *Liguria dsrB* sequences and BLASTp reference sequences was constructed with RAXML in ARB. Lost City *dsrB* sequences were present, but too short and thus could not be incorporated into the tree. Alignment was performed using ClustalW. CROMO and *Liguria* sequences are bold italic. The scale bar indicates 0.01 inferred amino acid substitutions per site and bootstrap values > 50% are shown at branch nodes. [Color figure can be viewed at wileyonlinelibrary.com]

hypothetical concentrations (1 nM to 1 mM) constrain the possible dynamics of thiosulfate cycling in this system, similar to an approach previously applied to hydrogen oxidation in hot springs (Spear *et al.*, 2005). Thiosulfate oxidation is thermodynamically favourable across this entire range, for all oxidants considered in our calculations. At 1 μ M thiosulfate, thiosulfate oxidation coupled to nitrate provides energy at values of $\Delta G = -758 \pm 14 \text{ kJ}/(\text{mol S}_2\text{O}_3^{2-})$, and thiosulfate oxidation coupled to oxygen with energy levels equal to $\Delta G = -825 \pm 25 \text{ kJ}/(\text{mol S}_2\text{O}_3^{2-})$ (Supporting Information Tables S7 and S8). Microbial populations such as Ca. 'Serpentinomonas' (Suzuki *et al.*, 2014), members of Rhodobacterales (Tourova *et al.*, 2013) and Rhodocyclaceae (Meyer *et al.*, 2007) can facilitate the oxidation of thiosulfate to sulfate using components of the SOX pathway. SOX is highly expressed in three

CROMO wells, and the sulfate end-product potentially provides an energy source for the sulfate-reducing microbial community.

MAG data for thiosulfate oxidation pathways discussed here show that MAGs for *Hydrogenophaga* in CSWold host the complete pathway for thiosulfate oxidation via SOX, whereas two MAGs related to the Rhodobacteraceae host partial SOX pathways (Seyler *et al.*, 2020). Populations within the genera *Dethiobacter* (Clostridia) identified by *PhyloPythiaS+* are likely to mediate thiosulfate disproportionation, as these capabilities have been recorded in recent genome sequencing and physiological studies of these taxa (Sorokin *et al.*, 2011; Poser *et al.*, 2013; Melton *et al.*, 2017). The 3-mercaptopyruvate sulfurtransferase (*sseA*) and thiosulfate sulfurtransferase (*glpE*) genes encoding thiosulfate disproportionation to thiocyanate and sulfite are detected throughout CROMO (Fig. 4). The *sseA* gene is actively

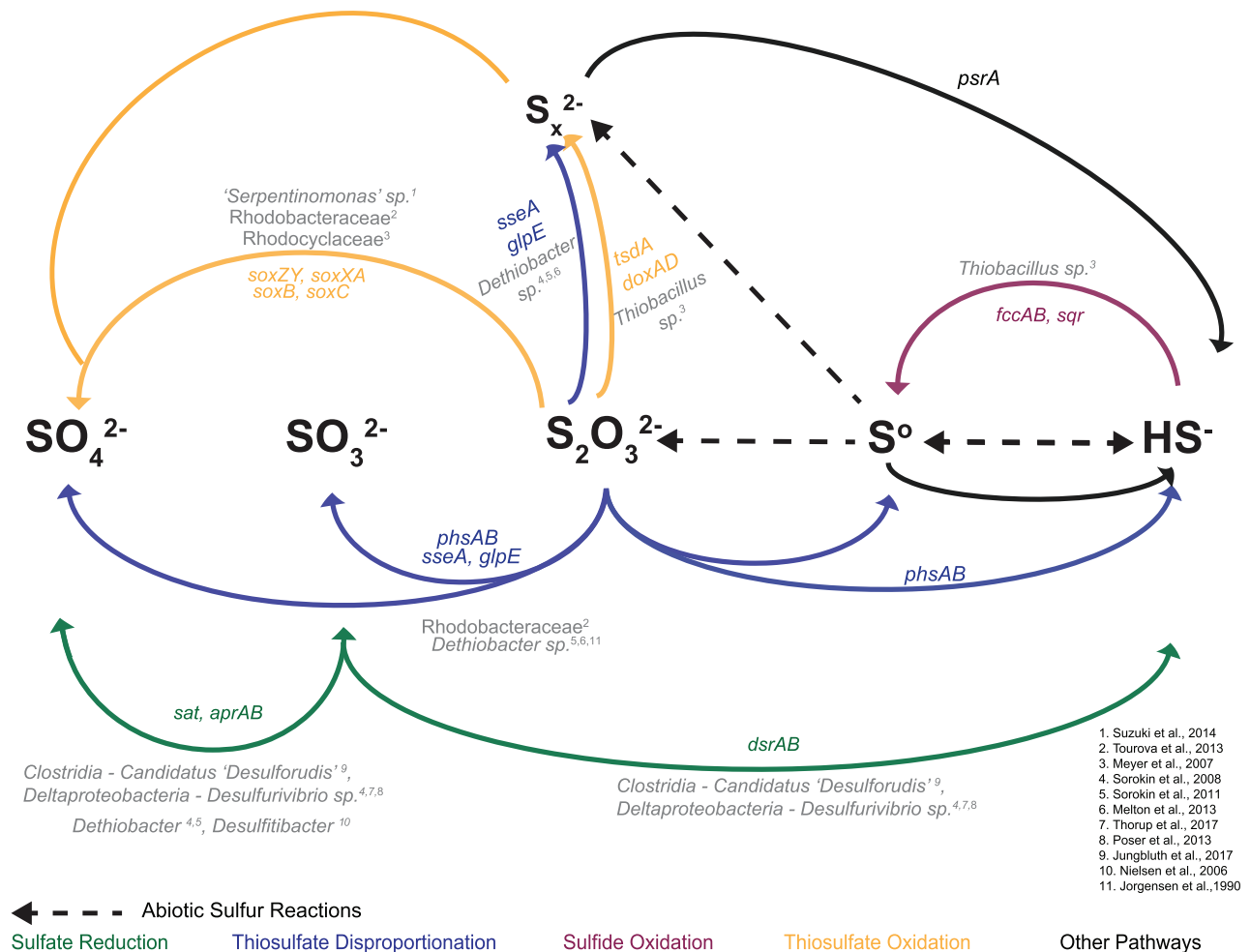


Fig. 6. Schematic showing how sulfur compounds can be cycled both biotically (coloured arrows) and abiotically (dashed arrows) within the most saline well at CROMO. Genes related to a particular metabolic pathway are noted above the corresponding arrow in matching colours, with organisms identified in this study annotated in grey beneath certain segments of metabolic pathways. [Color figure can be viewed at wileyonlinelibrary.com]

transcribed on multiple contigs predominantly in the two deepest and most saline wells, CSWold (71.23 FPKM) and N08-B (188.53 FPKM), though it is ubiquitous at CROMO. *Desulfitispora* has also been shown to utilize thiosulfate, sulfite and elemental sulfur as electron acceptors (Sorokin and Muyzer, 2010) and may be involved with the cycling of these compounds.

High rates of thiosulfate reduction at moderate salinities were detected in organisms isolated from alkaline soda lakes (Sorokin et al., 2011). At CROMO, thiosulfate reduction rates have not been determined, but the reactions would be favourable across a wide range of possible thiosulfate concentrations. Thiosulfate reduction to sulfide coupled to formate oxidation generates Gibbs energy yields in the range of -150 ± 25 kJ/(mol $S_2O_3^{2-}$) of available energy, and thiosulfate reduction coupled to acetate, methane or hydrogen provides energy of $\Delta G = -80$ to -210 kJ/(mol $S_2O_3^{2-}$) (Supporting Information Tables S7

and S8). Organisms may facilitate these reactions that in turn could stimulate symbiotic networks between organisms and promote microbial activity within this extreme ecosystem, similar to what has been observed in Precambrian shield subsurface environments (Lau et al., 2016).

The thermodynamic and genomic data presented here suggest potential for pervasive metabolism of intermediate and reduced sulfur compounds in the serpentinization-influenced CROMO groundwater. Throughout a hypothetical six-order of magnitude range in concentration, thiosulfate would react with favourable Gibbs energy change in a variety of oxidation, reduction and disproportionation reactions (Supporting Information Table S8). These reactions correspond to metabolic potential associated with some of the most abundant microbial populations at the site and could serve to underpin microbial productivity and ecosystem structure.

It is important to note that due to the overlapping nature of sulfur cycling reactions, there are likely more intricate relationships occurring that keep intermediate compounds at low levels and that cannot be easily detected with the methods used here. However, the intermediate sulfur species examined in thermodynamic calculations and metagenomic analyses can serve to regenerate HS⁻ or SO₄²⁻, thereby maintaining both reduced and oxidized sulfur pools and continuing the cycle.

Potential for serpentinizing ophiolites to preserve aspects of their marine origin

The process of ophiolite genesis and emplacement onto continental margins serves to transport ultramafic rock, marine sediments, organic matter and seawater to the terrestrial environment. These effects are evident in the sodium and chloride chemistry measured at CROMO and several other well-studied serpentinite groundwaters (Neal and Shand, 2002; Cipolli *et al.*, 2004; Monnin *et al.*, 2014) that likely impact microbial ecosystem structure and influence the biogeochemistry of these sites. To investigate this, we compare CROMO (81.9 mM Cl⁻ and 73.9 mM Na⁺ in CSWold) to the low-salinity, sub-aerial serpentinizing springs of the Voltri Massif in Liguria, Italy (650 µM Cl⁻ and 550 µM Na⁺ in Rio Leone; Chavagnac *et al.*, 2013) and to the deep-sea LCHF located near the Mid-Atlantic Ridge (Kelley *et al.*, 2005). At the Voltri Massif, the ultrabasic fluids retain sulfate concentrations ranging from 0.5 to 32.8 µM (Chavagnac *et al.*, 2013), and sulfide concentrations around 16.2–18.7 µM (Brazelton *et al.*, 2017). The LCHF chimneys host a gradient of water chemistries influenced by seawater as one endmember and hyperalkaline, hydrogen- and methane-rich vent fluids as the other. Sulfate in these hydrothermal fluids ranges from 1000 to 4000 µM (Kelley *et al.*, 2005; Supporting Information Table S2) and sulfide varies from 245 to 2880 µmol kg⁻¹ (Lang *et al.*, 2012). As both sites host measurable sulfate and sulfide, a suite of metabolisms related to sulfur cycling is likely within the serpentinite-hosted communities.

At CROMO, Lost City and Liguria, normalized abundances of key genes involved in sulfur cycling confirm that microbial populations are capable of cycling sulfur through four metabolic processes: sulfate reduction, sulfide oxidation, thiosulfate disproportionation and thiosulfate oxidation (Fig. 4; Supporting Information Tables S10 and S11). As seen through this study, at CROMO both oxidative and reductive components of the sulfur cycle are represented. At Lost City, where reduced hydrothermal fluids circulate through chimneys out to oxidized seawater, genes for oxidative processes, such as thiosulfate oxidation (SOX complex; 150.02–954.83 FPKM) and

sulfide oxidation (*sqr*; 23.32–1281.73 FPKM at H08 site) are abundant (Fig. 4). At LCHF, genes for sulfate reduction processes are also present (*sat* = 6.75–247.90 FPKM; *aprAB* = 4.63–17.57 FPKM; *dsrAB* = 9.53–66.98 FPKM), but at lower levels. As Liguria is a freshwater-influenced site sampled from hydrothermal springs, the system is less-isolated from the atmosphere and anoxic water at depth can mix with oxygenated compounds near the surface. Overall, genes for sulfur cycling at Liguria are generally lower than the peak values at CROMO and LCHF (Fig. 4; Supporting Information Table S10). Results from this study suggest that there are differences in the microbial sulfur cycle between serpentinizing systems (Fig. 4) and that these variations are likely explained by niche-specific differences (e.g., vigorous hydrologic flow at a hydrothermal chimney system compared to ophiolitic groundwater) that influence the concentration and availability of sulfur compounds. On the seafloor, where reduced fluids actively vent into oxidized seawater, there is a stark chemical gradient between reduced, actively venting hyperalkaline fluids and sulfate-rich seawater that influence the microbial communities and genes transcribed. In ophiolite complexes, where a range of seawater volumes can be retained and mix over a multitude of time scales, these serpentinizing systems can range in salinity from fresh to saline. CROMO fluids are brackish and sulfur-rich, and Liguria fluids are lower in both salinity and concentrations of dissolved sulfur compounds, as described above. The varying hydrologies and impact upon fluid chemistry may strongly influence the composition of resident microbial communities.

The new observations from this study are supported by recent work from other serpentinizing ecosystems. Recent biogeochemical studies show that formate oxidation, likely carried out by sulfate reducing bacteria, supports the base of the LCHF ecosystem (Lang *et al.*, 2018). At the Prony Hydrothermal Field in New Caledonia, a hybrid between marine and terrestrial serpentinites, sulfur-cycling organisms similar to the strictly anaerobic *Dethiobacter alkaliphilus* were identified that can utilize acetate and sugars with elemental sulfur, polysulfides and thiosulfate, yet cannot reduce sulfate directly (Sorokin *et al.*, 2008; Pisapia *et al.*, 2017; Frouin *et al.*, 2018). For comparison, freshwater sites such as the Santa Elena ophiolite in Costa Rica and The Cedars in California lack sulfate (i.e., < 5.0 µM) and to date show little evidence of sulfur cycling (Crespo-Medina *et al.*, 2017). Similar to the versatility observed in carbon and H₂ cycling within serpentinite-hosted microbial populations (Brazelton *et al.*, 2012; Suzuki *et al.*, 2014), the ability to cycle sulfur compounds through multiple pathways lends flexibility to energy production as these systems change through time.

Taken together, our results point towards the microbial metabolic potential for extensive sulfur cycling within the brackish groundwater at CROMO. The elevated concentrations of sulfur compounds, considerable energetic incentive, diversity of sulfur-cycling organisms and elevated sulfur-cycling gene activity collectively suggest an important role for sulfur metabolisms in serpentinite groundwaters. We suggest that genera, such as *Dethiobacter*, *Desulfitispora* and the candidate genus '*Desulforudis*' are critical to this process within the brackish, sulfur-rich serpentinitizing fluids. Future studies should focus on quantifying the reactive, potentially short-lived intermediate sulfur species in serpentinitizing systems using techniques such as high-performance liquid chromatography (Findlay and Kamysny, 2017) or cyclic voltammetry (Boyd and Druschel, 2013), and incorporate these measurements of intermediate sulfur metabolisms into their experimental design. We expect that intermediate and oxidized sulfur species serve as important electron acceptors in oxidant-limited serpentinitizing groundwater and play important roles in constraining the bulk productivity of these systems. Additionally, as serpentinitizing ophiolites originate at the seafloor, we suggest that they serve as a vector to transport sulfur compounds and potentially sulfur-metabolizing microbes onto the continents. This in turn can impact the biogeographic distribution, evolution and composition of resident microbial communities. Continued comprehensive, genome-wide comparisons in populations across a range of serpentinitizing sites will serve to further illuminate the interplay of large-scale geologic processes and the geomicrobiology therein.

Experimental procedures

Aqueous geochemistry

All CROMO wells (CSW, QV, N08) were directly sampled for their biogeochemistry in July 2014. Fluids were pumped from discrete depths via positive displacement Teflon bladder pumps (Geotech Environmental Equipment, Denver, CO, USA) to the surface, where they were flushed through a YSI 3059 flow cell attached to a digital YSI multiprobe (Yellow Springs, OH, USA) for pH, oxidation-reduction potential (ORP), DO, specific conductance and temperature measurements once DO stabilized. Fluids were collected via tubing attached to the flow cell, which allowed syringes to directly sample water pumped anoxically from the well bottom. Aqueous samples were preserved for anion and cation analysis as described below, and dissolved gas (CH₄, CO, H₂), organic acid (acetate, lactate, propionate, formate) and DIC quantification according to previously published protocols in

Crespo-Medina and colleagues (2014) and Twing and colleagues (2017).

Well water was pumped and immediately filtered through a 0.22 µm Sterivex syringe filter (Millipore, Billerica, MA, USA) into sterile 15 ml Falcon tubes (Fisher Scientific) and stored at 4°C. Anions in CROMO fluids and analytical blanks were measured using a Dionex ICS-2100 Ion Chromatography System (ThermoScientific), generating data for the concentrations of chloride [limit of detection (LOD) 0.56 µM, uncertainty 2.7%], nitrite (LOD 2.17 µM, uncertainty 3.15%), nitrate (LOD 1.61 µM, uncertainty 2.2%), bromide (LOD 1.25 µM, uncertainty 4.0%), fluoride (LOD 1.05 µM, uncertainty 6.5%) and sulfate (LOD 1.56 µM, uncertainty 0.41%).

Hydrogen sulfide concentrations were determined via colorimetry according to previously published protocols for the methylene blue method (Cline, 1969; Joye *et al.*, 2004; Weber *et al.*, 2016; 1.0 µM LOD). Fluid samples (45 ml) from each well were preserved immediately in the field using 600 µl of a 20% zinc acetate solution to precipitate volatile sulfide in the form of solid zinc sulfide. Samples and standards were immediately run in parallel to a blank at 670 nm on an UV-1800 Shimadzu UV spectrophotometer at Michigan State University.

Cations were preserved in the field by addition of 600 µl of a 20% zinc acetate solution to 45 ml of sample fluid and stored at 4°C until analysis. Values reported (Supporting Information Table S1) are comparable to CROMO samples preserved in nitric acid (Sabuda and Cardace, unpublished data). Cation samples were sent to the Analytical Geochemistry Laboratory at the University of New Mexico for analysis and immediately run using an inductively coupled plasma optical emission spectrometer (ICP-OES) (Fig. 1). Sodium and chloride values are reported from serpentinitizing systems around the world, including those not mentioned in the text, but are referenced here (Culkin and Cox, 1966; Barnes *et al.*, 1978, 2015; Marques *et al.*, 2008; Blank *et al.*, 2009; Suda *et al.*, 2014; Cardace *et al.*, 2015; Meyer-Dombard *et al.*, 2015; Seyfried *et al.*, 2015; Boschetti *et al.*, 2017).

Gibbs energy calculations

Gibbs energy values for 18 potential energy-yielding reactions involving the various states of sulfur speciation (Supporting Information Tables S7 and S8) were calculated based on the measured fluid compositions (Supporting Information Table S1). Formate and acetate values were estimated based on previous sampling trips for these calculations and estimated as 1.0 µM if data were not available for a particular well. It is critical to note that thiosulfate concentrations were not directly measured and instead were estimated at 1.0 nM, µM and mM for this study (Jorgensen, 1990; Thamdrup *et al.*, 1994).

Sensitivity calculations were performed to span three orders of magnitude, 1.0 nM, 1.0 μM and 1.0 mM $\text{S}_2\text{O}_3^{2-}$. Speciation calculations were performed to determine activities of dissolved species for each sample using Geochemist's Workbench® (Aqueous Solutions LLC, Champaign, IL, USA). The amount of energy available from each metabolic reaction was calculated according to previous work by Amend and Shock (2001):

$$\Delta G_r = \Delta G_r^0 + RT \ln Q \quad (1)$$

where ΔG_r is the Gibbs energy of reaction, ΔG_r^0 is the standard Gibbs energy, R is the universal gas constant, T is the temperature in Kelvin and Q is the reaction quotient of activities of the compounds involved in the reaction. The reaction quotient incorporated activities calculated from the speciation models and reaction stoichiometries. ΔG_r^0 values for the selected reactions were obtained from Amend and Shock (2001). Finally, the amount of energy available in each parcel of fluid was estimated by multiplying ΔG_r by the concentration of the limiting reactant divided by its stoichiometric coefficient (McCollom and Shock, 1997).

Extraction of DNA and RNA

In concert with aqueous geochemistry and cell enumeration preservations, 4 L of fluids from CROMO wells were pumped from each well bottom and immediately filtered through Sterivex 0.2 μm filter cartridges (Millipore, Billerica, MA, USA) using a portable peristaltic pump. Cartridges were kept on ice during filtration, immediately stored in liquid nitrogen upon completion, shipped to the home laboratory and stored at -80°C until processing. Total genomic DNA extractions were completed as previously described by Brazelton and colleagues (2017), Crespo-Medina and colleagues (2017), and Twing and colleagues (2017) and briefly described here. Freeze/thaw cycles and lysozyme/Proteinase K treatment were performed to lyse cells, followed by purification with phenol-chloroform, precipitation using ethanol and purification using QiaAmp (Qiagen, Hilden, Germany) columns according to manufacturer instructions. A Qubit 2.0 fluorometer (ThermoFisher) was used to quantify extracted DNA using a Qubit dsDNA High Sensitivity Assay kit.

Extractions for RNA from CROMO wells were performed as described previously with slight modifications (Lin and Stahl, 1995; Macgregor *et al.*, 1997). Briefly, frozen 0.2 μm Sterivex filter cartridges were broken open, cut into four equal pieces and divided into two screw-cap Eppendorf tubes containing phenol, 20% sodium dodecyl sulfate, 5 \times low-pH buffer, and 0.2–0.5 g baked zirconium beads. Samples were bead-beaten for 3 min, heated in a

60 $^\circ\text{C}$ water bath for 10 min, bead beaten again for 3 min and centrifuged at 4 $^\circ\text{C}$ and 18,407 $\times g$ to separate phases. Supernatant was transferred to a fresh Eppendorf tube and chilled. 1 \times low-pH buffer was added to the remaining sample, and bead-beating was repeated. Supernatants were combined, and phenol, 1:1 phenol : chloroform and chloroform were added in series with vortexing and centrifugation in between. Between steps, aqueous phases were transferred to clean Eppendorf tubes. The final aqueous phase was transferred to a clean Eppendorf tube with additions of ammonium acetate, isopropanol and magnesium chloride before vortexing and incubation at -20°C overnight. Samples were centrifuged for 30 min at 4 $^\circ\text{C}$, washed with ethanol and dried under vacuum before suspension in RNase-free water and storage at -80°C until analysed.

Bacterial 16S rRNA amplicon sequencing and data analysis

Purified DNA from CROMO wells was submitted to the Genomics Core Facility at Michigan State University for processing using an Illumina MiSeq instrument. The V4 region of the 16S rRNA gene (515F/806R primers) was amplified using dual indexed Illumina fusion primers (Kozich *et al.*, 2013). An Invitrogen SequelPrep DNA Normalization Plate was then used to normalize and pool the products. The pool was loaded on an Illumina MiSeq v2 flow cell and sequenced using a standard 500 cycle reagent kit after library quality control and quantitation was performed. Illumina Real Time Analysis (RTA) software v1.18.54 performed base calling. The RTA output was demultiplexed and converted to FastQ files using Illumina Bcl2fastq v1.8.4.

USEARCH 8 (Edgar, 2010) was then used to filter and merge paired-end sequence reads. Additional quality filtering was performed to remove sequences with ambiguous bases and more than eight homopolymers using mothur (Schloss *et al.*, 2009), and chimaeras were removed with mothur's implementation of UCHIME (Edgar *et al.*, 2011). The sequences were pre-clustered with the mothur command pre.cluster (diffs = 1), which reduced the number of unique sequences from 362,039 to 211,847. The pre.cluster step removes rare sequences most likely created by sequencing errors (Schloss and Westcott, 2011). These pre-clustered sequences were used as operational taxonomic units (OTUs) for all downstream analyses.

Sequences were aligned to the SILVA SSURef alignment (v132), and taxonomic classifications were assigned using mothur (Pruesse *et al.*, 2007; Schloss *et al.*, 2009), as described in Twing *et al.*, 2017. The counts for each OTU were normalized to the total number of reads for each sample. Following this, normalized

counts were averaged for wells that had more than one representative sample to negate statistical issues related to pseudoreplication (Kuhar, 2006). In order to perform Pearson correlation analyses, the data were then filtered to retain OTUs that made up greater than 1% of any given sample which resulted in 82 unique OTUs to be used specifically for statistical analyses. The resulting 82 OTUs were combined into a data table along with geochemical data collected during sampling to analyse relationships between abundant species and environmental parameters.

Statistical information

A two-tailed Pearson correlation coefficient matrix was computed with the `rcor.test` function in the R package `ltm` (Rizopoulos, 2006) using 16S rRNA OTU relative abundances > 1% and aqueous chemical data for all CROMO wells. Correlation coefficients were filtered to remove values that did not have *p*- and *q* values of 0.05 or less. Pairwise correlations that fit these criteria were included in further analyses and used to guide investigations between environmental parameters and specific OTUs (Supporting Information Tables S4–S6).

The non-metric multidimensional scaling plot was created using count data for all 16S rRNA OTU relative abundances in each sample and the Morisita-Horn distance metric in R (R Core Team, 2019) (v.3.5.1) with the `Phyloseq` package (McMurdie and Holmes, 2013). With this metric, statistically significant environmental parameters (*p* values ≤ 0.05) were subsequently plotted as overlying vectors in R using the `vegan` package (v. 2.5–3) (Oksanen *et al.*, 2018).

Metagenomic sample preparation, sequencing and data analysis

Samples were submitted to the Joint Genome Institute (JGI) for metagenomic and metatranscriptomic sequencing on an Illumina HiSeq2000 instrument. At the JGI, a Covaris LE220 ultrasonicator was used to shear DNA samples into 270 bp fragments, and size selection was performed using SPRI beads. DNA fragments were end-repaired, A-tailed, and ligated with Illumina-compatible adapters with barcodes unique for each library. KAPA Biosystem's next-generation sequencing library qPCR kit and Roche LightCycler 280 RT PCR instrument were used to quantify libraries. Ten library pools were assembled and prepared for Illumina sequencing in one lane each. Clustered flowcells were produced using a TruSeq paired-end cluster kit (v3) and Illumina's cBot instrument. The Illumina HiSeq2000 instrument was utilized with a TruSeq SBS sequencing kit (v3) and a 2 × 150 indexed run recipe to sequence the samples. The raw sequence

reads were trimmed by the JGI with a minimum quality score cutoff of 10 to remove adapters. These trimmed reads from CROMO wells were previously reported by Twing and colleagues (2017), but additional quality-filtering and a new assembly, distinct from the JGI assembly reported by Twing and colleagues (2017) was performed for this study.

The trimmed reads from the JGI were subjected to an additional quality screen to trim 3' adapters with `cutadapt` v. 1.15 (Martin, 2011), to remove replicate sequences, and to trim sequences again with a threshold of 20 along a sliding window of 6 bases with `qtrim` v. 2.0.2 (Shrestha *et al.*, 2014). All CROMO metagenomes and metatranscriptomes were pooled together for a master CROMO assembly computed with `Ray Meta` v.2.3.1 (Boisvert *et al.*, 2012), and short reads were mapped to the assembly using `Bowtie2` v.2.2.6 (Langmead and Salzberg, 2013). Phylogenetic affiliation of contigs was assigned using `PhyloPythiaS+` (Gregor *et al.*, 2016), and the `Prokka` pipeline (Seemann, 2014) was used for gene prediction and functional annotation of contigs. The arguments – metagenome and – proteins were used with `Prokka` v.1.12 (Seemann, 2014) to indicate that genes should be predicted with the implementation of `Prodigal` v.2.6.2 (Hyatt *et al.*, 2010) optimized for metagenomes as described by Twing *et al.*, 2017. All details for MAG assembly and datasets are reported in the methods of Seyler and colleagues (2020).

Predicted protein-coding sequences were annotated by searching the Kyoto Encyclopedia of Genes and Genomes (KEGG) (Ogata *et al.*, 1999) release v. 83.2 within `Prokka`. `HTSeq` v.0.6.1 was used to calculate predicted protein abundances (Anders *et al.*, 2015), and the abundances of predicted protein functions in all CROMO metagenomes and metatranscriptomes were normalized to predicted protein size and metagenome size. Data reported here are in units of metagenome fragments per kilobase of predicted protein sequence per million mapped reads (FPKM). Detailed documentation of all metagenomic data processing is provided on the Brazelton lab's website (<https://baas-becking.biology.utah.edu/data/category/18-protocols>), and all custom software and scripts are available at <https://github.com/Brazelton-Lab>.

Phylogenies of genes of interest were constructed by first aligning predicted coding sequences against the NCBI NR database (v. 2017-06-07), and using the top two BLASTP protein hits for each predicted sequence. BLASTP hits all had E-values > 1e–136. The lowest percent identity for the top two hits was 56.6% (`PROKKA_587390`) and only 4 hits had percent identities < 75%. The highest percent identity was 98.6% (`PROKKA_192589`), and 15 hits had percent identities > 90%. The remainder fell between 70% and 90%. Predicted protein sequences and their respective top two

BLASTP hits were aligned using Clustal Omega (Sievers *et al.*, 2014) to produce a FASTA file for use in creation of phylogenetic trees. A 1000-bootstrap maximum likelihood phylogenetic tree of *dsrB* was computed with RAxML in ARB (Ludwig *et al.*, 2004) using the Dayhoff substitution model. CROMO, Lost City and Liguria *dsrB* sequences and their top two BLASTP reference sequences were aligned using the ClustalW protein alignment (slow and accurate) option in ARB. Sequences were then filtered to equal lengths, and sequences less than 352 amino acids in length were excluded. This cutoff eliminated Lost City sequences. The scale bar indicates 0.01 inferred amino acid substitutions per site, and a bootstrap cutoff value of 50% was utilized.

Sequence data availability

The 16S rRNA sequence data from CROMO are publicly available in the NCBI Sequence Read Archive under project number PRJNA289273. CROMO metagenome sequences were previously published by Twing and colleagues (2017) and are publicly available in the JGI IMG/M database under the project IDs: 1021918, 1,021,921, 1,021,924 and 1,021,927; and in the MG-RAST database under the following sample IDs: 4569549.3, 4569550.3, 4569551.3 and 4569552.3. CROMO metatranscriptome sequences are publicly available in the NCBI Sequence Read Archive under the following Accession IDs: SRX3339504, SRX3339503, SRX3339089, SRX3331179, SRX3331177, SRX3330963, SRX3330943 and SRX3330753. Metagenomic data from Liguria, Italy and the Lost City Hydrothermal Field were published previously by Brazelton and colleagues (2017) and Lang and colleagues (2018) respectively.

Acknowledgements

We thank C. Koehler and P. Aigner at the UC-Davis McLaughlin Natural Reserve, and the Homestake Mining Company for support with CROMO field work and in the establishment of CROMO respectively. We thank M. Crespo-Medina for laboratory RNA extractions and K. Twing for collecting field samples. We acknowledge A. Ali at the University of New Mexico for ICP-OES analyses, and S. Ruhala and T. Hampton at Michigan State University for performing IC analyses. This work was supported by the NASA Astrobiology Institute CAN-7 Rock Powered Life (RPL) Grant #NNA15BB02A, and the Alfred P. Sloan Foundation's Deep Carbon Observatory (2011-12-01). All of the sequencing was performed by the DOE Joint Genome Institute (supported by the Office of Science of the U.S. Department of Energy under the contract DE-AC02-05CH11231). We also thank D. Morgan-Smith, K. Twing, D. Long, L. Seyler, K. Kashefi and J. Zarnetske for insightful discussions related to this work.

Author contributions

M.C.S. and M.O.S. created and designed the study. M.C.S., M.D.Y.K., L.I.P. and D.C. performed field sampling at CROMO. M.C.S. and M.D.Y.K. processed and analysed all geochemical data. W.J.B. prepared and assembled metagenomic and metatranscriptomic data that M.C.S. later analysed. L.I.P. performed statistical analyses on geochemical and microbiological data and assisted in the creation of figures. T.M.M. made thermodynamic calculations with information provided by M.C.S. T.M.H. made critical edits and provided insight to thermodynamic calculations. M.C.S. wrote the manuscript and created final figures and tables with input and discussion from M.O.S., L.I.P., T.M.H., W.J.B., T.M.M., M.D.Y.K. and D.C.

Competing financial interest

The authors declare no competing financial interests.

Data availability

Correspondence and requests for materials should be addressed to M.O.S.

References

- Alcalá, F.J., and Custodio, E. (2008) Using the Cl/Br ratio as a tracer to identify the origin of salinity in aquifers in Spain and Portugal. *J Hydrol* **359**: 189–207.
- Amend, J.P., and Shock, E.L. (2001) Energetics of overall metabolic reactions of thermophilic and hyperthermophilic Archaea and bacteria. *FEMS Microbiol Rev* **25**: 175–243.
- Anders, S., Pyl, P.T., and Huber, W. (2015) HTSeq-A Python framework to work with high-throughput sequencing data. *Bioinformatics* **31**: 166–169.
- Barnes, I., Oneil, J.R., and Trescases, J.J. (1978) Present day serpentinization in New Caledonia, Oman and Yugoslavia. *Geochim Cosmochim Acta* **42**: 144–145.
- Barnes, I., Lamarche, V.C., and Himmelberg, G. (2015) Geochemical evidence of present-day serpentinization. *Science* **156**: 830–832.
- Blank, J.G., Green, S.J., Blake, D., Valley, J.W., Kita, N.T., Treiman, A., and Dobson, P.F. (2009) An alkaline spring system within the Del Puerto Ophiolite (California, USA): a Mars analog site. *Planet Space Sci* **57**: 533–540.
- Boisvert, S., Raymond, F., Godzaridis, E., Laviolette, F., and Corbeil, J. (2012) Ray Meta: scalable de novo metagenome assembly and profiling. *Genome Biol* **13**: R122.
- Boschetti, T., Toscani, L., Iacumin, P., and Selmo, E. (2017) Oxygen, hydrogen, boron and lithium isotope data of a natural spring water with an extreme composition: a fluid from the dehydrating slab? *Aquat Geochem* **23**: 299–313.
- Boyd, E.S., and Druschel, G.K. (2013) Involvement of intermediate sulfur species in biological reduction of elemental

- sulfur under acidic, hydrothermal conditions. *Appl Environ Microbiol* **79**: 2061–2068.
- Brazelton, W.J., Schrenk, M.O., Kelley, D.S., and Baross, J. A. (2006) Methane- and sulfur-metabolizing microbial communities dominate the Lost City hydrothermal field ecosystem. *Appl Environ Microbiol* **72**: 6257–6270.
- Brazelton, W.J., Nelson, B., and Schrenk, M.O. (2012) Metagenomic evidence for H₂ oxidation and H₂ production by serpentinite-hosted subsurface microbial communities. *Front Microbiol* **2**: 1–16.
- Brazelton, W.J., Thornton, C.N., Hyer, A., Twing, K.I., Longino, A.A., Lang, S.Q., et al. (2017) Metagenomic identification of active methanogens and methanotrophs in serpentinite springs of the Voltri Massif, Italy. *PeerJ* **5**: e2945.
- Cardace, D., and Hoehler, T.M. (2009) Serpentinizing fluids craft microbial habitat. *Northeast Nat* **4**: 133–144.
- Cardace, D., Hoehler, T., McCollom, T., Schrenk, M., Carnevale, D., Kubo, M., and Twing, K. (2013) Establishment of the Coast Range ophiolite microbial observatory (CROMO): drilling objectives and preliminary outcomes. *Sci Drill* **16**: 45–55.
- Cardace, D., Meyer-Dombard, D.R., Woycheese, K.M., and Arcilla, C.A. (2015) Feasible metabolisms in high pH springs of the Philippines. *Front Microbiol* **6**: 10.
- Chavagnac, V., Monnin, C., Ceuleneer, G., Boulart, C., and Hoareau, G. (2013) Characterization of hyperalkaline fluids produced by low-temperature serpentinization of mantle peridotites in the Oman and Ligurian ophiolites. *Geochem Geophys Geosyst* **14**: 2496–2522.
- Chivian, D., Brodie, E.L., Alm, E.J., Culley, D.E., Dehal, P. S., DeSantis, T.Z., et al. (2008) Environmental genomics reveals a single-species ecosystem deep within Earth. *Science* **322**: 275–278.
- Cipolli, F., Gambardella, B., Marini, L., Ottonello, G., and Zuccolini, M.V. (2004) Geochemistry of high-pH waters from serpentinites of the Gruppo di Voltri (Genova, Italy) and reaction path modeling of CO₂ sequestration in serpentinite aquifers. *Appl Geochem* **19**: 787–802.
- Cline, J.D. (1969) Spectrophotometric determination of hydrogen sulfide in natural waters. *Limnol Oceanogr* **14**: 454–458.
- Crespo-Medina, M., Twing, K.I., Kubo, M.D.Y., Hoehler, T. M., Cardace, D., McCollom, T., and Schrenk, M.O. (2014) Insights into environmental controls on microbial communities in a continental serpentinite aquifer using a microcosm-based approach. *Front Microbiol* **5**: 604.
- Crespo-Medina, M., Twing, K.I., Sánchez-Murillo, R., Brazelton, W.J., McCollom, T.M., and Schrenk, M.O. (2017) Methane dynamics in a tropical serpentinizing environment: the Santa Elena Ophiolite, Costa Rica. *Front Microbiol* **8**: 1–14.
- Culkin, F., and Cox, R.A. (1966) Sodium, potassium, magnesium, calcium and strontium in sea water. *Deep-Sea Res Oceanogr Abstr* **13**: 789–804.
- Dilek, Y., and Furnes, H. (2011) Ophiolite genesis and global tectonics: geochemical and tectonic fingerprinting of ancient oceanic lithosphere. *Bull Geol Soc Am* **123**: 387–411.
- Edgar, R.C. (2010) Search and clustering orders of magnitude faster than BLAST. *Bioinformatics* **26**: 2460–2461.
- Edgar, R.C., Haas, B.J., Clemente, J.C., Quince, C., and Knight, R. (2011) UCHIME improves sensitivity and speed of chimera detection. *Bioinformatics* **27**: 2194–2200.
- Findlay, A.J., and Kamysshny, A. (2017) Turnover rates of intermediate sulfur species (S_x²⁻, S₀, S₂O₃²⁻, S₄O₆²⁻, SO₃²⁻) in anoxic freshwater and sediments. *Front Microbiol* **8**: 1–15.
- Fones, E.M., Colman, D.R., Kraus, E.A., Nothaft, D.B., Poudel, S., Rempfert, K.R., et al. (2019) Physiological adaptations to serpentinization in the Samail Ophiolite, Oman. *ISME J* **13**: 1750–1762.
- Frouin, E., Bes, M., Ollivier, B., Quéméneur, M., Postec, A., Debroas, D., et al. (2018) Diversity of rare and abundant prokaryotic phylotypes in the Prony hydrothermal field and comparison with other serpentinite-hosted ecosystems. *Front Microbiol* **9**: 1–13.
- Gregor, I., Dröge, J., Schirmer, M., Quince, C., and McHardy, A.C. (2016) *PhyloPythiaS+*: a self-training method for the rapid reconstruction of low-ranking taxonomic bins from metagenomes. *PeerJ* **4**: e1603.
- Heling, D., and Schwarz, A. (2007) Iowait in serpentinite muds at sites 778, 779, 780, and 784: a possible cause for the low chlorinity of pore waters. *Proc Ocean Drill Program Sci Results* **125**: 313–323.
- Hem, J.D. (1985) *Study and Interpretation of the Chemical Characteristics of Natural Water*. Washington, DC: United States Geological Survey, p. 255.
- Hyatt, D., Chen, G.-L., Locascio, P.F., Land, M.L., Larimer, F.W., and Hauser, L.J. (2010) Prodigal: prokaryotic gene recognition and translation initiation site identification. *BMC Bioinformatics* **11**: 119.
- Jorgensen, B.B. (1990) A thiosulfate shunt in the sulfur cycle of marine sediments. *Science* **249**: 152–154.
- Joye, S.B., Boetius, A., Orcutt, B.N., Montoya, J.P., Schulz, H.N., Erickson, M.J., and Lugo, S.K. (2004) The anaerobic oxidation of methane and sulfate reduction in sediments from Gulf of Mexico cold seeps. *Chem Geol* **205**: 219–238.
- Jungbluth, S.P., Glavina del Rio, T., Tringe, S.G., Stepanauskas, R., and Rappé, M.S. (2017) Genomic comparisons of a bacterial lineage that inhabits both marine and terrestrial deep subsurface systems. *PeerJ* **5**: 1–22.
- Katz, B.G., Eberts, S.M., and Kauffman, L.J. (2011) Using Cl/Br ratios and other indicators to assess potential impacts on groundwater quality from septic systems: a review and examples from principal aquifers in the United States. *J Hydrol* **397**: 151–166.
- Kelley, D.S., Karson, J.A., Früh-green, G.L., Yoerger, D.R., Shank, T.M., Butterfield, D.A., et al. (2005) A serpentinite-hosted ecosystem: the Lost City Hydrothermal Field. *Science* **307**: 1428–1434.
- Kozich, J.J., Westcott, S.L., Baxter, N.T., Highlander, S.K., and Schloss, P.D. (2013) Development of a dual-index sequencing strategy and curation pipeline for analyzing amplicon sequence data on the miseq illumina sequencing platform. *Appl Environ Microbiol* **79**: 5112–5120.
- Kuhar, C.W. (2006) In the deep end: pooling data and other statistical challenges of zoo and aquarium research. *Zoo Biol* **25**: 339–352.
- Lang, S.Q., Früh-Green, G.L., Bernasconi, S.M., Lilley, M.D., Proskurowski, G., Méhay, S., and Butterfield, D.A. (2012)

- Microbial utilization of abiogenic carbon and hydrogen in a serpentinite-hosted system. *Geochim Cosmochim Acta* **92**: 82–99.
- Lang, S.Q., Früh-Green, G.L., Bernasconi, S.M., Brazelton, W.J., Schrenk, M.O., and McGonigle, J.M. (2018) Deeply-sourced formate fuels sulfate reducers but not methanogens at Lost City hydrothermal field. *Sci Rep* **8**: 755.
- Langmead, B., and Salzberg, S.L. (2013) Fast gapped-read alignment with Bowtie 2. *Nat Methods* **9**: 357–359.
- Lau, M.C.Y., Kieft, T.L., Kulooy, O., Linage-Alvarez, B., van Heerden, E., Lindsay, M.R., *et al.* (2016) An oligotrophic deep-subsurface community dependent on syntrophy is dominated by sulfur-driven autotrophic denitrifiers. *Proc Natl Acad Sci U S A* **113**: E7927–E7936.
- Leavitt, W.D., Cummins, R., Schmidt, M.L., Sim, M.S., Ono, S., Bradley, A.S., and Johnston, D.T. (2014) Multiple sulfur isotope signatures of sulfite and thiosulfate reduction by the model dissimilatory sulfate-reducer, *Desulfovibrio alaskensis* str. G20. *Front Microbiol* **5**: 1–16.
- Lin, C., and Stahl, D.A. (1995) Taxon-specific probes for the cellulolytic genus *Fibrobacter* reveal abundant and novel equine-associated populations. *Appl Environ Microbiol* **61**: 1348–1351.
- Ludwig, W., Strunk, O., Westram, R., Richter, L., Meier, H., Yadhukumar, A., *et al.* (2004) ARB: a software environment for sequence data. *Nucleic Acids Res* **32**: 1363–1371.
- Luther, G.W., Findlay, A.J., MacDonald, D.J., Owings, S.M., Hanson, T.E., Beinart, R.A., and Girguis, P.R. (2011) Thermodynamics and kinetics of sulfide oxidation by oxygen: a look at inorganically controlled reactions and biologically mediated processes in the environment. *Front Microbiol* **2**: 1–9.
- McCollom, T.M., and Seewald, J.S. (2013) Serpentinites, hydrogen, and life. *Elements* **9**: 129–134.
- McCollom, T.M., and Shock, E.L. (1997) Geochemical constraints on chemolithoautotrophic metabolism by microorganisms in seafloor hydrothermal systems. *Geochim Cosmochim Acta* **61**: 4375–4391.
- Macgregor, B.J., Moser, D.P., Alm, E.W., Nealson, K.H., and Stahl, D.A. (1997) Crenarchaeota in Lake Michigan sediment. *Appl Environ Microbiol* **63**: 1178–1181.
- McMurdie, P.J., and Holmes, S. (2013) Phyloseq: an R package for reproducible interactive analysis and graphics of microbiome census data. *PLoS One* **8**: e61217.
- Marques, J.M., Carreira, P.M., Carvalho, M.R., Matias, M.J., Goff, F.E., Basto, M.J., *et al.* (2008) Origins of high pH mineral waters from ultramafic rocks, Central Portugal. *Appl Geochem* **23**: 3278–3289.
- Martin, M. (2011) Cutadapt removes adapter sequences from high-throughput sequencing reads. *EMBnet J* **17**: 10–12.
- Melton, E.D., Sorokin, D.Y., Overmars, L., Lapidus, A.L., Pillay, M., Ivanova, N., *et al.* (2017) Draft genome sequence of *Dethiobacter alkaliphilus* strain AHT1T, a gram-positive sulfidogenic polyextremophile. *Stand Genomic Sci* **12**: 1–9.
- Meyer, B., Imhoff, J.F., and Kuever, J. (2007) Molecular analysis of the distribution and phylogeny of the *soxB* gene among sulfur-oxidizing bacteria - evolution of the Sox sulfur oxidation enzyme system. *Environ Microbiol* **9**: 2957–2977.
- Meyer-Dombard, D.R., Woycheese, K.M., Yargicoglu, E.N., Cardace, D., Shock, E.L., Gulecal-Pektas, Y., and Temel, M. (2015) High pH microbial ecosystems in a newly discovered, ephemeral, serpentinitizing fluid seep at Yanartas (Chimera), Turkey. *Front Microbiol* **6**: 1–13.
- Miller, H.M., Matter, J.M., Kelemen, P., Ellison, E.T., Conrad, M.E., Fierer, N., *et al.* (2016) Modern water/rock reactions in Oman hyperalkaline peridotite aquifers and implications for microbial habitability. *Geochim Cosmochim Acta* **179**: 217–241.
- Monnin, C., Chavagnac, V., Boulart, C., Menez, B., Gerard, M., Gerard, E., *et al.* (2014) Fluid chemistry of the low temperature hyperalkaline hydrothermal system of Prony Bay (New Caledonia). *Biogeosciences* **11**: 5687–5706.
- Morrill, P.L., Kuenen, J.G., Johnson, O.J., Suzuki, S., Rietze, A., Sessions, A.L., *et al.* (2013) Geochemistry and geobiology of a present-day serpentinitization site in California: The Cedars. *Geochim Cosmochim Acta* **109**: 222–240.
- Müller, A.L., Kjeldsen, K.U., Rattei, T., Pester, M., and Loy, A. (2015) Phylogenetic and environmental diversity of DsrAB-type dissimilatory (bi)sulfite reductases. *ISME J* **9**: 1152–1165.
- Neal, C., and Shand, P. (2002) Spring and surface water quality of the Cyprus ophiolites. *Hydrol Earth Syst Sci* **6**: 797–817.
- Ogata, H., Goto, S., Sato, K., Fujibuchi, W., and Bono, H. (1999) KEGG: Kyoto Encyclopedia of Genes and Genomes. *Nucleic Acids Res* **27**: 29–34.
- Oksanen, J., Blanchet, F.G., Kindt, R., Legendre, P., Minchin, P.R., O'Hara, R.B., *et al.* (2018) *Vegan: community ecology package, vR package version 2.5-3*. URL <http://CRAN.R-project.org/package=vegan>.
- Ortiz, E., Tominaga, M., Cardace, D., Schrenk, M.O., Hoehler, T.M., Kubo, M.D., and Rucker, D.F. (2018) Geophysical characterization of serpentinite hosted hydrogeology at the McLaughlin Natural Reserve, Coast Range Ophiolite. *Geochem Geophys Geosyst* **19**: 114–131.
- Osburn, M.R., LaRowe, D.E., Momper, L.M., and Amend, J. P. (2014) Chemolithotrophy in the continental deep subsurface: Sanford underground research facility (SURF), USA. *Front Microbiol* **5**: 1–14.
- Peters, E.K. (1993) D-¹⁸O enriched waters of the Coast Range Mountains, northern California: connate and ore-forming fluids. *Geochim Cosmochim Acta* **57**: 1093–1104.
- Pisapia, C., Gérard, E., Gérard, M., Lecourt, L., Lang, S.Q., Pelletier, B., *et al.* (2017) Mineralizing filamentous bacteria from the Prony Bay hydrothermal field give new insights into the functioning of serpentinitization-based subseafloor ecosystems. *Front Microbiol* **8**: 1–18.
- Poser, A., Lohmayer, R., Vogt, C., Knoeller, K., Planer-Friedrich, B., Sorokin, D., *et al.* (2013) Disproportionation of elemental sulfur by haloalkaliphilic bacteria from soda lakes. *Extremophiles* **17**: 1003–1012.
- Pruesse, E., Quast, C., Knittel, K., Fuchs, B.M., Ludwig, W., Peplies, J., and Glöckner, F.O. (2007) SILVA: a comprehensive online resource for quality checked and aligned ribosomal RNA sequence data compatible with ARB. *Nucleic Acids Res* **35**: 7188–7196.

- Quéméneur, M., Bes, M., Postec, A., Mei, N., Hamelin, J., Monnin, C., et al. (2014) Spatial distribution of microbial communities in the shallow submarine alkaline hydrothermal field of the Prony Bay, New Caledonia. *Environ Microbiol Rep* **6**: 665–674.
- R Core Team (2019). *R: A Language and Environment for Statistical Computing*. Vienna, Austria: R Foundation for Statistical Computing. URL <https://www.R-project.org/>.
- Rempfert, K.R., Miller, H.M., Bompard, N., Nothhaft, D., Matte, J.M., Kelemen, P., et al. (2017) Geological and geochemical controls on subsurface microbial life in the Samail Ophiolite, Oman. *Front Microbiol* **8**: 1–21.
- Rizopoulos, D. (2006) ltm: an R package for latent variable modeling and item response theory analyses. *J Stat Softw* **17**: 1–25.
- Schink, B. (1997) Energetics of syntrophic cooperation in methanogenic degradation. *Microbiol Mol Biol Rev* **61**: 262–280.
- Schloss, P.D., and Westcott, S.L. (2011) Assessing and improving methods used in operational taxonomic unit-based approaches for 16S rRNA gene sequence analysis. *Appl Environ Microbiol* **77**: 3219–3226.
- Schloss, P.D., Westcott, S.L., Ryabin, T., Hall, J.R., Hartmann, M., Hollister, E.B., et al. (2009) Introducing mothur: open-source, platform-independent, community-supported software for describing and comparing microbial communities. *Appl Environ Microbiol* **75**: 7537–7541.
- Schrenk, M.O., Brazelton, W.J., and Lang, S.Q. (2013) Serpentinization, carbon, and deep life. *Rev Mineral Geochem* **75**: 575–606.
- Schwarzenbach, E.M., Früh-Green, G.L., Bernasconi, S.M., Alt, J.C., Shanks, W.C., Gaggero, L., et al. (2012) Sulfur geochemistry of peridotite-hosted hydrothermal systems: comparing the Ligurian ophiolites with oceanic serpentinites. *Geochim Cosmochim Acta* **91**: 283–305.
- Schwarzenbach, E.M., Gill, B.C., Gazel, E., and Madrigal, P. (2016) Sulfur and carbon geochemistry of the Santa Elena peridotites: comparing oceanic and continental processes during peridotite alteration. *Lithos* **252–253**: 92–108.
- Seemann, T. (2014) Prokka: rapid prokaryotic genome annotation. *Bioinformatics* **30**: 2068–2069.
- Seyfried, W.E., Pester, N.J., Tutolo, B.M., and Ding, K. (2015) The Lost City hydrothermal system: constraints imposed by vent fluid chemistry and reaction path models on seafloor heat and mass transfer processes. *Geochim Cosmochim Acta* **163**: 59–79.
- Seyler, L.M., Brazelton, W.J., McLean, C., Putman, L.I., Hyer, A., Kubo, M.D.Y., et al. (2020) Carbon assimilation strategies in ultrabasic groundwater: clues from the integrated study of a serpentinization-influenced aquifer. *mSystems* **5**: 1–17.
- Shrestha, R.K., Lubinsky, B., Bansode, V.B., Moins, M.B.J., McCormack, G.P., and Travers, S.A. (2014) QTrim: a novel tool for the quality trimming of sequence reads generated using the Roche/454 sequencing platform. *BMC Bioinformatics* **15**: 1–6.
- Sievers, F., Wilm, A., Dineen, D., Gibson, T.J., Karplus, K., Li, W., et al. (2014) Fast, scalable generation of high-quality protein multiple sequence alignments using Clustal Omega. *Mol Syst Biol* **7**: 539–539.
- Sorokin, D.Y., and Muyzer, G. (2010) Haloalkaliphilic spore-forming sulfidogens from soda lake sediments and description of *Desulfitispora alkaliphila* gen. nov., sp. nov. *Extremophiles* **14**: 313–320.
- Sorokin, D.Y., Tourova, T.P., Mußmann, M., and Muyzer, G. (2008) *Dethiobacter alkaliphilus* gen. nov. sp. nov., and *Desulfurivibrio alkaliphilus* gen. nov. sp. nov.: two novel representatives of reductive sulfur cycle from soda lakes. *Extremophiles* **12**: 431–439.
- Sorokin, D.Y., Tourova, T.P., Kolganova, T.V., Detkova, E.N., Galinski, E.A., and Muyzer, G. (2011) Culturable diversity of lithotrophic haloalkaliphilic sulfate-reducing bacteria in soda lakes and the description of *Desulfonatronum thioautotrophicum* sp. nov., *Desulfonatronum thiosulfatophilum* sp. nov., *Desulfonatronovibrio thiodismutans* sp. nov., and *Desulfonatronovibrio magnus* sp. nov. *Extremophiles* **15**: 391–401.
- Sousa, D.Z., Visser, M., van Gelder, A.H., Boeren, S., Pieterse, M.M., Pinkse, M.W.H., et al. (2018) The deep-subsurface sulfate reducer *Desulfotomaculum kuznetsovii* employs two methanol-degrading pathways. *Nat Commun* **9**: 239.
- Spear, J.R., Walker, J.J., Mccollom, T.M., and Pace, N.R. (2005) Hydrogen and bioenergetics in the Yellowstone geothermal ecosystem. *Proc Natl Acad Sci U S A* **102**: 2555–2560.
- Suda, K., Ueno, Y., Yoshizaki, M., Nakamura, H., Kurokawa, K., Nishiyama, E., et al. (2014) Origin of methane in serpentinite-hosted hydrothermal systems: the CH₄-H₂-H₂O hydrogen isotope systematics of the Hakuba Happo hot spring. *Earth Planet Sci Lett* **386**: 112–125.
- Suzuki, S., Kuene, J.G., Schipper, K., van der Velde, S., Ishii, S., Wu, A., et al. (2014) Physiological and genomic features of highly alkaliphilic hydrogen-utilizing Betaproteobacteria from a continental serpentinizing site. *Nat Commun* **5**: 3900.
- Thamdrup, B., Finster, K., Fossing, H., Hansen, J.W., and Jørgensen, B.B. (1994) Thiosulfate and sulfite distributions in porewater of marine sediments related to manganese, iron, and sulfur geochemistry. *Geochim Cosmochim Acta* **58**: 67–73.
- Thorup, C., and Schramm, A. (2017) Disguised as a sulfate reducer: growth of the Deltaproteobacterium *Desulfurivibrio alkaliphilus* by sulfide oxidation with nitrate. *mBio* **8**: 1–9.
- Tiago, I., and Verissimo, A. (2013) Microbial and functional diversity of a subterrestrial high pH groundwater associated to serpentinization. *Environ Microbiol* **15**: 1687–1706.
- Tourova, T.P., Slobodova, N.V., Bumazhkin, B.K., Kolganova, T.V., Muyzer, G., and Sorokin, D.Y. (2013) Analysis of community composition of sulfur-oxidizing bacteria in hypersaline and soda lakes using *soxB* as a functional molecular marker. *FEMS Microbiol Ecol* **84**: 280–289.
- Twing, K.I., Brazelton, W.J., Kubo, M.D.Y., Hyer, A.J., Cardace, D., Hoehler, T., et al. (2017) Serpentinization-influenced groundwater harbors extremely low diversity microbial communities adapted to high pH. *Front Microbiol* **8**: 308.
- Van Den Bosch, P.L.F., Sorokin, D.Y., Buisman, C.J.N., and Janssen, A.J.H. (2008) The effect of pH on thiosulfate formation in a biotechnological process for the removal of

hydrogen sulfide from gas streams. *Environ Sci Technol* **42**: 2637–2642.

Wasmund, K., Mußmann, M., and Loy, A. (2017) The life sulfuric: microbial ecology of sulfur cycling in marine sediments. *Environ Microbiol Rep* **9**: 323–344.

Weber, H.S., Thamdrup, B., and Habicht, K.S. (2016) High sulfur isotope fractionation associated with anaerobic oxidation of methane in a low-sulfate, iron-rich environment. *Front Earth Sci* **4**: 1–14.

Woycheese, K.M., Meyer-Dombard, D.R., Cardace, D., Argayosa, A.M., and Arcilla, C.A. (2015) Out of the dark:

transitional subsurface-to-surface microbial diversity in a terrestrial serpentinizing seep (Manleluag, Pangasinan, The Philippines). *Front Microbiol* **6**: 1–12.

Supporting Information

Additional Supporting Information may be found in the online version of this article at the publisher's web-site:

Appendix S1: Supporting Information